



PERGAMON

Scripta Materialia 47 (2002) 101–106



www.actamat-journals.com

# Superplasticity in a rolled Mg–3Al–1Zn alloy by two-stage deformation method

J.C. Tan, M.J. Tan \*

*School of Mechanical and Production Engineering, Nanyang Technological University, Nanyang Avenue, Singapore 639798, Singapore*

Received 13 February 2002; accepted 15 April 2002

## Abstract

A two-stage deformation method is proposed to enhance the superplasticity of a rolled Mg–3Al–1Zn alloy. In the first stage, fine grains capable of grain boundary sliding are attained through dynamic recrystallization while the second stage is performed at a higher temperature to take advantage of these fine grains. © 2002 Acta Materialia Inc. Published by Elsevier Science Ltd. All rights reserved.

*Keywords:* Superplasticity; Magnesium alloys; Mg–3Al–1Zn; Dynamic recrystallization

## 1. Introduction

Magnesium alloys have poor formability and limited ductility at room temperature attributed to their hexagonal close-packed (HCP) crystal structure. As a result, to date, the formed products of magnesium and its alloys are scarce [1]. Because of its extreme lightness, the use of magnesium alloy in structural applications will be highly successful if the formability can be improved. The low density makes it highly viable for rapidly moving components and allows thicker sections to be utilized, hence simplifying the design and manufacturing processes.

Earlier work by the present authors [2] found that the optimum deformation conditions of Mg–

3Al–1Zn were at 450 °C and  $2 \times 10^{-4} \text{ s}^{-1}$ , attaining a maximum elongation ( $\delta$ ) of 265% and strain rate sensitivity ( $m$ -value) of 0.3, which signifies a Class-I solid solution alloy. Even though the specimen initially possessed a relatively fine microstructure ( $\approx 12 \mu\text{m}$ ), it eventually coarsened due to grain growth during deformation at elevated temperature. It was found that the resultant coarse-grained microstructure governed the type of predominant deformation mechanism and the accommodation process. Therefore, by changing the deformation mechanism, greater  $\delta$  can be attained if the grain structure can be refined via dynamic recrystallization (DRX).

Recently, it has been reported by Mohri et al. [3] that superplasticity of a rolled Mg–9Al–1Zn (AZ91) alloy can be substantially improved by refining the grains through DRX. The use of DRX in enhancing superplasticity of several other superplastic materials such as Al–Mg alloys [4,5], Al 2219 [6], Al 7475 [7,8],  $\text{Co}_3\text{Ti}$  [9] and Duralumin [10]

\* Corresponding author. Tel.: +65-6790-5582; fax: +65-6791-1859.

E-mail address: [mmjtan@ntu.edu.sg](mailto:mmjtan@ntu.edu.sg) (M.J. Tan).

have been reported by several other authors. Superplastic forming of a material with fine grains requires less applied force since the flow stress decreases as grain size is reduced, therefore contributing towards energy as well as cost savings.

## 2. Experimental procedures

The magnesium alloy used in this study was a commercial Mg–3Al–1Zn (AZ31B-O) cross-rolled sheet with a chemical composition of Mg–3.0%Al–1.0%Zn–0.2%Mn–0.02%Si (in wt.%). The as-received material had an average grain size of 12  $\mu\text{m}$  determined using the linear intercept method [11]. Tensile specimens with a gauge of 15 mm length, 4 mm width and 2 mm thickness were electro-discharged machined with the tensile axes oriented parallel to the final rolling direction.

The elevated temperature tensile tests were performed in an Instron-4206 universal testing machine equipped with electrical resistance furnace which can maintain a temperature variation of  $\pm 2$  K. The tests were performed in air at atmospheric pressure and employing constant strain rates. All tests were conducted by first heating up each specimen to the desired temperature, followed by a 20 min holding time to ensure thermal equilibrium. Prior to straining, the temperature of the specimen was further verified using a thermocouple put in contact with the gauge of the specimen. The variation of stress and strain was monitored continuously by a personal computer equipped with an automatic data acquisition system. In order to preserve the microstructures, at the specified strain or at fracture, specimens were immediately

unloaded and quenched in water. Specimens for optical microscopy were sectioned, cold mounted, polished and then etched in acetic picral (5 ml acetic acid + 6 g picric acid + 10 ml  $\text{H}_2\text{O}$  + 100 ml ethanol (95%)). The scanning electron microscope (SEM) was employed to investigate the surface morphology.

## 3. Results

In the proposed “two-stage deformation” method, the first stage (stage I) of deformation is aimed at refining the coarse microstructure through DRX, while the second stage (stage II) is carried out at the optimum conditions for superplastic deformation of coarse-grained Mg–3Al–1Zn, i.e.  $1 \times 10^{-4} \text{ s}^{-1}$  at 400  $^\circ\text{C}$  and  $2 \times 10^{-4} \text{ s}^{-1}$  at 450  $^\circ\text{C}$  [2]. Table 1 depicts the results of the elevated temperature tests performed using single and two-stage methods.

The optimum DRX condition for stage I was at 250  $^\circ\text{C}$  and  $1 \times 10^{-4} \text{ s}^{-1}$  up to 60% of deformation, determined by investigating the evolution of DRX microstructures at various stages of deformation, as shown in Fig. 1. At the beginning of the deformation process, (a)  $\varepsilon = 0.05$ , as a result of static grain growth during heating-up process, the as-received microstructure transformed into coarse-grained structure whose average size was  $\approx 25 \mu\text{m}$ . At (b)  $\varepsilon = 0.18$ , the coarser grain boundaries appeared serrated while small amount of fine recrystallized grains started to nucleate along the grain boundaries and at triple junctions. When (c)  $\varepsilon = 0.37$ , DRX grains encompassed the original coarser grain boundaries but the microstructure

Table 1

Experimental conditions and elongation-to-failure for specimens tested using single and two-stage deformations

Specimen no.	Test temperature ( $^\circ\text{C}$ )	Strain rate ( $\text{s}^{-1}$ )	Elongation (%) <sup>a</sup>	Elongation-to-failure, $\pm 5\%$
1	250	$1 \times 10^{-4}$	–	140
2	400	$1 \times 10^{-4}$	–	250
3	250 $\rightarrow$ 400	$1 \times 10^{-4}$	60	320
4	450	$2 \times 10^{-4}$	–	265
5	250 $\rightarrow$ 450	$1 \times 10^{-4} \rightarrow 2 \times 10^{-4}$	60	360

All specimens were tested at constant strain rates.

<sup>a</sup> Elongation where temperature or/and strain rate change occurred. The time required for raising the temperature from stage I to II was about 10 min.

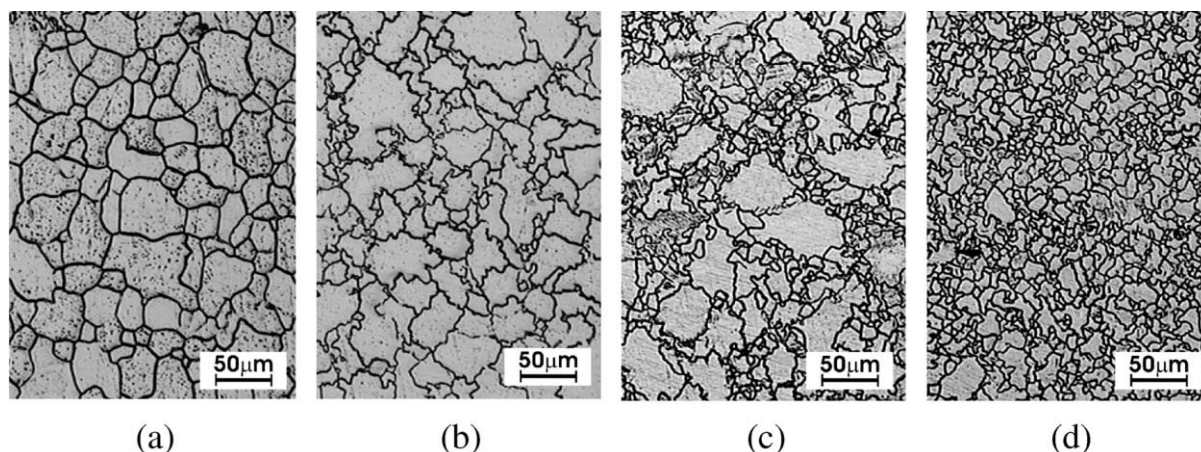


Fig. 1. Micrographs depicting typical microstructural evolutions at true strain,  $\varepsilon$ , of (a) 0.05, (b) 0.18, (c) 0.37 and (d) 0.47 for DRX specimens tested at 250 °C and constant strain rate of  $1 \times 10^{-4} \text{ s}^{-1}$ . Tensile axes were horizontal.

remained inhomogeneous. At (d)  $\varepsilon = 0.47$ , high volume fraction ( $\approx 85\%$ ) of fine grains with an average size of  $6 \mu\text{m}$  was attained.

Although Specimen 1 was deformed at optimum DRX conditions and possessed a high volume fraction of recrystallized grains, its elongation-to-failure was limited to 140% due to cavitation. Specimen 2 was independently deformed at 400 °C and  $1 \times 10^{-4} \text{ s}^{-1}$ , achieving  $\delta$  of 250% and a coarse-grained microstructure. Specimen 3 was tested using the two-stage deformation method. It was first deformed at 250 °C, followed by a temperature increase to 400 °C at 60% strain. The strain rate remained constant at  $1 \times 10^{-4} \text{ s}^{-1}$  throughout the test. This specimen attained a total elongation (i.e. sum of the first and second stages) of 320%, which was a 70% improvement over the independently strained Specimen 2. The specimen failed by necking (Fig. 2b) implying that the dynamically recrystallized fine grains experienced grain growth at 400 °C and therefore resulted in plastic necking. Another positive effect of grain refinement is the reduction of flow stress during steady state deformation. Under the same deformation conditions, the flow stress was originally at  $\approx 14.5 \text{ MPa}$  (Fig. 3b) in the single stage test, but was reduced to  $\approx 9 \text{ MPa}$  in the two-stage test (Fig. 3c). The reduction in flow stress can be ascribed to the presence of finer grains and hence grain

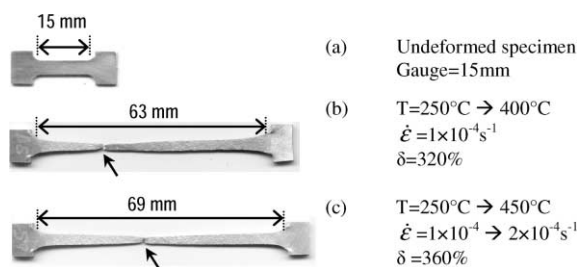


Fig. 2. Specimens of the two-stage deformation method: (a) undeformed specimen with initial gauge length of 15 mm. (b) Specimen 3 failed at 320%, employing stage I: 250 °C,  $1 \times 10^{-4} \text{ s}^{-1}$  to 60%; followed by stage II: 400 °C,  $1 \times 10^{-4} \text{ s}^{-1}$  until fracture. (c) Specimen 5 fractured at 360%, employing stage I: 250 °C,  $1 \times 10^{-4} \text{ s}^{-1}$  to 60%; followed by stage II: 450 °C,  $2 \times 10^{-4} \text{ s}^{-1}$ . All specimens failed by necking, as indicated by the arrows.

boundary sliding (GBS) mechanism was operational.

Specimen 5 was initially deformed at the optimum DRX conditions. Subsequently, the temperature was raised to 450 °C and the constant strain rate was increased to  $2 \times 10^{-4} \text{ s}^{-1}$ . Fig. 4(b) illustrates the aforementioned deformation procedure, while Fig. 2(c) depicts the fractured specimen. The conditions chosen for stage II corresponded to the optimum temperature and strain rate for maximum elongation-to-failure in a single stage test, as shown in Fig. 4(a). By comparing the true stress–strain

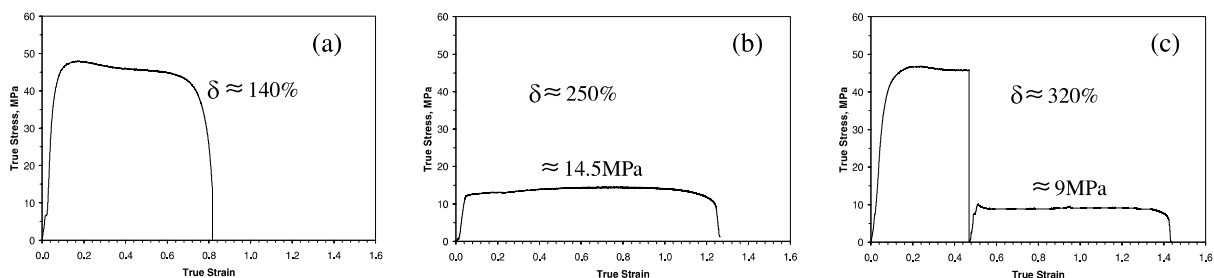


Fig. 3. True stress–strain curves showing the effects of temperature change during high temperature deformation. All tests were performed at a constant strain rate of  $1 \times 10^{-4} \text{ s}^{-1}$ . Two tests were conducted independently for (a) Specimen 1 at 250 °C and (b) Specimen 2 at 400 °C. Whilst (c) Specimen 3 was tested using two-stage deformation at 250 °C for stage I up to 60% elongation, followed by stage II at 400 °C.

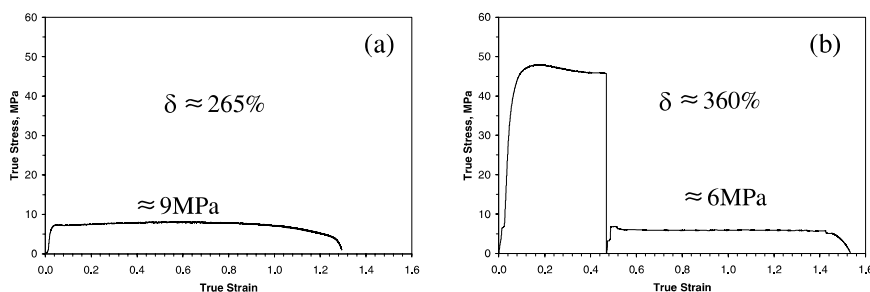


Fig. 4. True stress–strain curves showing the effects of temperature and strain rate change during high temperature deformation: (a) Specimen 4 was tested at 450 °C,  $2 \times 10^{-4} \text{ s}^{-1}$  and (b) Specimen 5 was strained using two-stage deformation at 250 °C,  $1 \times 10^{-4} \text{ s}^{-1}$  for the first stage up to a strain of 60%, followed by the second stage at 450 °C,  $2 \times 10^{-4} \text{ s}^{-1}$ . All tests were performed at constant strain rates.

curves in Fig. 4, it is evident that  $\delta$  was substantially enhanced from 265% to 360% and concurrently, the flow stress was reduced from 9 to 6 MPa. In addition, it is interesting to note that the deformation curve during stage II exhibited a relatively steady state flow behavior. This again can be attributed to the high percentage of fine and homogeneous grains that deformed by GBS.

#### 4. Discussion

During stage I, a high volume fraction of fine grains was generated after 60% of deformation (Fig. 1d), therefore the first stage corresponded primarily to the development of fine grains by DRX. In addition, stage I was conducted up to only 60% and not higher in order to prevent the nucleation of cavities that will substantially reduce

the tensile elongation during stage II. As a result of fine grains development, a small stress decrease was detected (Fig. 3a), but not as large as had been reported for a Mg–9Al–1Zn alloy [3]. During the early part of stage II ( $\delta < 100\%$ ), the fine grains were deforming by GBS (Fig. 5a), accommodated by intragranular slip and grain boundary diffusion. The GBS mechanism was verified by conducting a step strain rate test utilizing the Backofen Method [12], where the  $m$ -value was found to be  $\approx 0.5$ .

Experimental results also showed that there was a transition period between stage I and II, which occurred within  $100\% < \delta < 150\%$ . The microstructure was a combination of fine and coarse grains (Fig. 5b). The coarser grains originate from the initially fine grains which had grown when exposed to the higher temperature. Step strain rate test performed within this stage found that the  $m$ -value  $\approx 0.4$ . It is interesting to note that the

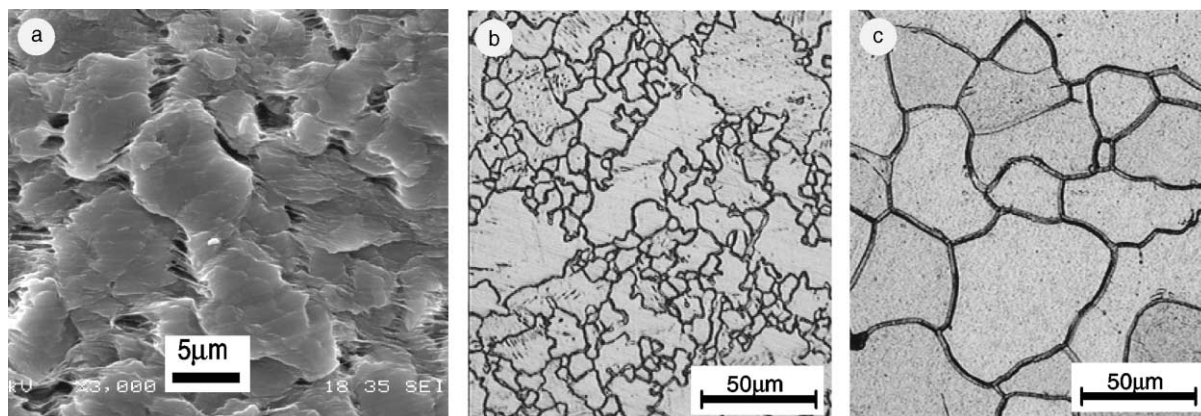


Fig. 5. (a) A typical SEM micrograph depicting GBS in the dynamically recrystallized grains in the early part ( $\delta < 100\%$ ) of stage I. Typical optical micrographs showing (b) a combination of fine and coarse grains structure in the transition stage ( $100\% < \delta < 150\%$ ) and (c) coarse grains found in the later part ( $\delta > 150\%$ ) of stage II. The specimens were deformed at stage I: 250 °C,  $1 \times 10^{-4} \text{ s}^{-1}$  to 60%, followed by stage II: 450 °C,  $2 \times 10^{-4} \text{ s}^{-1}$ .

$m$ -value was within 0.3 and 0.5, implying that the deformation mechanism could be a combination of GBS and viscous glide mechanisms, since the finer grains are capable of GBS whereas the coarser grains deform by viscous glide. This finding is also consistent with the work by Zelin et al. [13] involving the interaction of high temperature deformation mechanisms in a Mg–1.5%Mn–0.3%Ce magnesium alloy containing mixed fine and coarse grains.

At the later part of stage II ( $\delta > 150\%$ ), grain growth occurred due to the higher deformation temperature and accordingly altering the predominant deformation mechanism. Since the coarse-grained microstructure (Fig. 5c) does not permit GBS, a viscous glide mechanism accommodated by lattice diffusion is predominant. Step strain rate test performed within this stage found that the  $m$ -value was  $\approx 0.33$ , hence confirming viscous glide as the predominant mechanism [14–17]. This is also in good agreement with the plastic necking mode of failure (Fig. 2) attributed to the relatively low  $m$ -value. In addition, it is interesting to note that the flow stress (Fig. 3b) did not increase even at the later part ( $\delta > 150\%$ ) of deformation where GBS was no longer operational. This could be attributed to the viscous glide mechanism that is generally not very sensitive to grain size.

## 5. Conclusions

1. The proposed two-stage deformation method is effective in enhancing the elongation-to-failure for a rolled Mg–3Al–1Zn alloy. By employing this method, the maximum elongation attainable at 400 and 450 °C was improved from 250% and 265% to 320% and 360%, respectively.
2. Stage I is aimed at refining the coarse microstructure into fine equiaxial grains. The optimum DRX condition was identified as 250 °C at a constant strain rate of  $1 \times 10^{-4} \text{ s}^{-1}$ .
3. Stage II is performed at a higher temperature and is designed to take advantage of the fine grains obtained from stage I. GBS is operational in the earlier part of deformation due to the fine grains but viscous glide mechanism becomes predominant at the later part when the microstructure coarsens due to grain growth.

## References

- [1] Takuda H, Yoshii T, Hatta N. J Mater Proc Tech 1999; 89–90:135.
- [2] Tan JC, Tan MJ. Mater. Sci. Eng. A, to be published.
- [3] Mohri T, Mabuchi M, Nakamura N, Asahina T, Iwasaki H, Aizawa T, et al. Mat Sci Eng A 2000;290:139.

- [4] Lee E-W, McNelley TR. *Mater Sci Eng* 1987;93:45.
- [5] Hales SJ, McNelley TR, McQueen HJ. *Met Trans* 1991; 22A:1037.
- [6] Sitdikov OS, Kaybyshev RO, Safarov IM, Mazurina IA. *Phys Metals Metall* 2001;92(3):270.
- [7] Yang X, Miura H, Sakai T. *Mater Sci Forum* 1999;304(3): 103.
- [8] Sakai T, Yang XY, Miura H. *Mater Sci Eng* 1997;234A: 857.
- [9] Takasugi T, Watanabe Y, Inoue H. *Scripta Mater* 2000;43: 485.
- [10] Novikov II, Portnoy VK, Titov AO, Belov DYu. *Scripta Mater* 2000;42:899.
- [11] Annual Book of ASTM Standards, Section 3: 03.01, E112– 96, p. 229, American Society of Testing and Materials, Philadelphia, PA, 1998.
- [12] Backofen WA, Turner IR, Avery DH. *ASM Trans Quart* 1964;57:980.
- [13] Zelin MG, Yang HS, Valiev RZ, Mukerjee AK. *Metall Trans* 1992;23A:3135.
- [14] Taleff EM, Lesuer DR, Wadsworth J. *Metall Mater Trans* 1996;27A:343.
- [15] Li F, Bae DH, Ghosh AK. *Acta Mater* 1997;45(9):3887.
- [16] Friedman PA, Ghosh AK. *Metall Trans* 1996;27A:3827.
- [17] Verma R, Friedman PA, Ghosh AK, Kim S, Kim C. *Metall Trans* 1996;27A:1889.